# On Field-To-Wire Coupling Versus Conducted Injection Techniques

**Ken Javor**
EMC Compliance
P.O. Box 14161
Huntsville, Alabama, USA

***Abstract.*** Since the inception of conducted injection techniques to model radiated susceptibility/immunity coupling, consider-able debate has ensued regarding its validity. This paper affirms the viewpoint of Szentkuti (1989), builds upon test results of Adams (1992) and Trout (1996), and discusses Perini's theoretical observations (1993, 1995A, 1995B). Analytical and test results are presented which further demonstrate under what spe-cific conditions conducted and radiated techniques can be correlated, and how the works of Adams, Trout, and Perini fit into the general problem of modeling field-to-wire coupling. At frequen-cies where transmission line and antenna effects are minimal, con-ducted immunity techniques provide excellent correlation with analytical and empirical predictions of radiated coupling. From a practical standpoint, conducted injection techniques provide realistic coupling at frequencies and amplitude levels that would be uneconomical to achieve with traditional radiated techniques.

## INTRODUCTION

Conducted immunity (CI) techniques, both inductive (bulk current injection - BCI) and capacitive (coupling-decoupling networks - CDN) are attempts to overcome some well-known deficiencies of radiated immunity (RI) test methods:

1) When circuit- or cable-under-test (CUT) dimensions are short relative to a wavelength, then coupling is proportional to CUT length-to-wavelength ratio. CUT may not be adequately excited when lengths shorter than that of typical installations are tested. Ability to inject correct excitation at frequencies which would require excessive power levels of an RI test set up is the single greatest advantage of the CI technique.

2) For repeatability as well as maximizing coupling, test antenna must illuminate CUT dimensions evenly. This means antenna must be at some minimum distance from CUT, and test chambers must be lined with anechoic material to yield repeatable test results. Because antenna-CUT separation is a function of antenna physical aperture to wavelength ratio, and because any type of rf absorber has a low frequency cutoff, any given size test chamber has a low frequency cutoff. Thus, economics come into play. For IEC 1000-4-6, these physical and economic constraints translate into a required frequency range of 80 MHz - 1 GHz, implemented with 3 m antenna-CUT separation, and a requirement for ferrite tile-lining. With a low frequency cutoff of 80 MHz, another tech-nique is necessary to stress the CUT in LF through VHF bands.

Some authors have taken exception to claims that CI techniques yield improved accuracy and repeatability with respect to radiated techniques. This paper:

1) Defines both a philosophical and theoretical basis for modeling field-to-wire (FTW) coupling physics. Conditions un-der which FTW effects can be accurately predicted are presented.

2) Discusses specific CI injection techniques. Modeling of coupler/decoupler network and current clamp injection tech-niques are compared to actual FTW coupling. Test and analytical techniques compare and contrast CI/RI coupling.

3) Lists and discusses objections made against CI techniques. The most serious of these are Adams' test and Perini's analytical results which show large disparities between CI and RI coupling at frequencies where cables are electrically long.

## TEST PHILOSOPHY

Any type of qualification/certification, in order to provide added value, must satisfy one of the two following criteria:

1) test method accurately models *in situ* product performance, or
2) test results define bounds on expected product performance.

Criterion 1) above is appropriate for defining and testing desired product performance, e.g., an antenna's gain, bandwidth, and power handling capability. But it is useless for radiated (emissions or immunity) testing because, as Szentkuti notes, RE/ RI arises from unwanted antennas (common mode coupling to cables, seams, and apertures) which can only be described statistically. It is not the intent, nor can it be, to accurately model in the test chamber what happens at each customer's site. Only the second option, a rea-sonable worst case envelope, may be defined. (Szentkuti, 1989)

Consider first that on an open area test site (OATS) it is required to adjust CUTs to maximize emissions. Also, that antenna elevation must be scanned to look for emission peaks. Clearly, the second approach listed above is being followed. Second, consider that Part 15 of Title 47 of the Code of Federal Regula-tions (USA) requires inclusion of instructions regarding possible rfi from device. Notwithstanding Part 15 certification, if it is found to cause rfi, such rfi must be ameliorated or the Part 15 device must cease to be used. Such an instruction would not be necessary if EMI limits were such that no rfi could possibly occur. But this approach is uneconomical. EMI limits mandated by law provide rfi-free operation in the majority of situations. A more apropos example is line impedance stabilization network (LISN) definition for conducted emission (CE) testing. A LISN is a lumped-element model of a power bus transmission line at radio frequencies. Few would argue that the asymptotic 50 Ω (or in some cases, 150 Ω) LISN impedance is a high fidelity model of every power bus in existence at any frequency up to 30 MHz. But the LISN has been found useful, nonetheless, as a standard which provides a reasonable worst case measurement of CE. Between EMI tests, which measure maximum emissions, and the limits themselves, which attempt to prevent rfi in most cases, the test philosophy is clearly one of establishing and bounding an envelope of reasonably worst case emissions. The only correla-tion required or of interest is at the envelope of emission peaks.

If a conducted (emission/immunity) test can measure/inject a quantity corresponding to a worst case radiated effect, then that conducted test is a suitable replacement for the radiated test.

## PHYSICS OF FIELD-TO-WIRE COUPLING

Modeling of field-to-wire coupling depends on how EUT is grounded. Mains-powered equipment used at work or home operates far from (a poorly defined) ground. At best, equipment connects to that ground via a green wire which, as part of a power cord, is an uncontrolled rf impedance. Figure 1a illustrates IEC-1000-4-3 set up, modeling above described ground scheme.

Wooden table supports test set up 0.8 m above ground and over 1 m from any other surface. In Figure 1a, entire test set up acts as wire antenna. Pick-up depends on test set up electrical length and parasitic capacitance to ground. Prediction of coupling to equip-ment-associated CUTs is best done in the IEC 1000-4-6 manner, that is, an open-circuit potential with a defined source impedance.

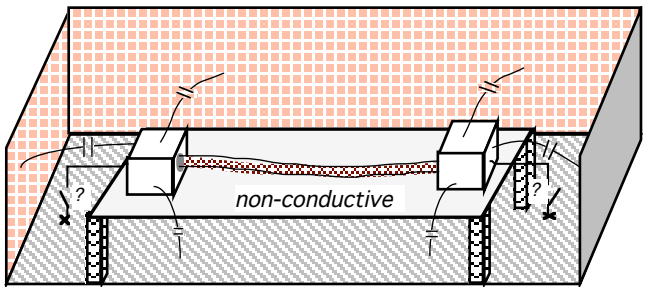


**Figure 1a:** *Radiated test set up, Class A/B products*

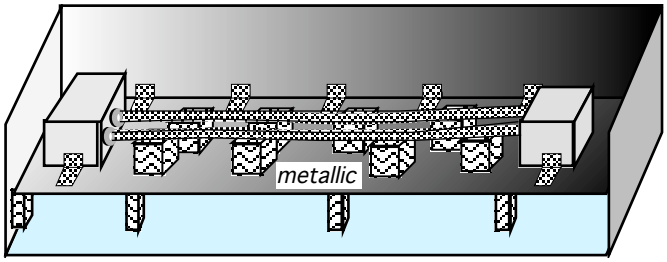


**Figure 1b:** *Radiated test set up, platform-installed equipment*

In contrast, equipment installed in vehicles (air, land, or sea-going), have well-defined relationships to platform ground, both in terms of resistance and proximity; hence, impedance. RI testing of such platform-installed equipment reflects the *in situ* condition. In Figure 1b, EUT is electrically bonded to a metallic tabletop which in turn is bonded to chamber surfaces. Wood or nonconductive blocks support CUTs 5 cm above ground, which is less than λ/10 even at 400 MHz, the highest frequency at which CI requirements are imposed. Cables thus connected are in such close proximity to ground that each individual cable bundle may be modeled as a single-wire-above-ground (swag) transmission line, and FTW coupling to such a transmission line may be accurately predicted. (Smith, 1977) In Figure 1b, two kinds of current are induced on transmission line. These are termed *antenna* and *loop* currents. In Figure 2, antenna currents are shown as unidirectional but variable in intensity along length of line, whereas loop currents are of relatively constant intensity and flow around loop. In contrast, only antenna currents are likely to be induced in the Figure 1a set up. Above discussion of antenna versus loop currents is instrumental in understanding differing mindsets of CI testing proponents. Platform design engineers view FTW common mode coupling to cables as in turn causing differential mode coupling to individual cable conductors and hence CUT-connected circuits within EUT. Engineers designing hardware for home, desktop, or industrial use see the EUT at the end of a wire antenna, and therefore the common mode recipient of whatever antenna currents are flowing. This explains IEC 1000-4-6 (1996) Figure 2a which is an illustration of above description.

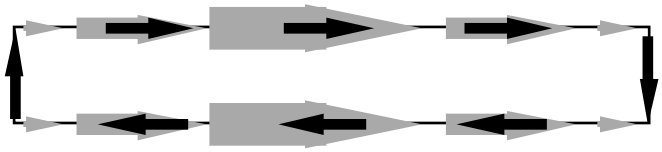

**Figure 2:** *Antenna (shaded) vs. loop (black) currents*

Differentiating between antenna and loop current is key to understanding many of the objections which have been raised relative to CI testing. Because CI techniques are required for commercial aircraft and automobiles, and all military platforms, analysis of the CUT as swag is important. Simple analyses are provided herein emphasizing physics of FTW coupling to transmission lines. The simple and useful case of a balanced two-wire line is reviewed. Analyses are worst case in that they calculate maximum potential coupled from a given electro-magnetic (em) wave. Maximum coupling efficiency derives from geometries where magnetic field penetrates loop plane at right angles and electric field component is parallel to either transmission line height or length. Happily, these configurations also simplify the mathematics to the maximum extent. First analysis treats an em wave of either horizontal or vertical (electric field) polarization, but with magnetic field penetrating plane of loop at a right angle, as shown in Figure 3.[1]

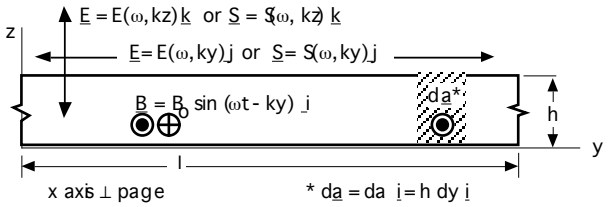


**Figure 3:** *Geometry for electromagnetic field coupling*

Faraday's Law (Maxwell integral form) states that voltage induced in a loop ($V_i$) is given equally by either line integral around loop or time rate of change of magnetic flux:

$$V_i = \oint \underline{E} \bullet d\underline{l} = -\frac{d}{dt} \int_{area} \underline{B} \bullet d\underline{a} \qquad (1)$$

where magnetic induction vector $\underline{B}$ (Tesla) = $\mu\underline{H}$, magnetic field (Amps/m) multiplied by free space permeability ($\mu = 4\pi \times 10^{-7}$ Henry/m), and $d\underline{a}$ is infinitesimal area over which magnetic induction field may be taken to be constant in both magnitude and direction. Because these equations calculate potential induced in a loop, currents associated with solutions to these equations are *loop* currents.

Maxwell's statement of Faraday in the form of (1) says that, once a particular magnetic field vector orientation relative to loop plane is determined, *induced voltage is invariant relative to available choices for Poynting vector orientation*, subject to plane wave definitions of Poynting vector ($\underline{S}$) and field impedance.

Derivation of transmission line effective height based on magnetic field is now presented. Electric field derivation is much simpler, and is only described qualitatively.

Magnetic component of traveling em wave in Figure 3 is

$$B = B_O \sin(\omega t - ky) = B_O \sin 2\pi(ft - \frac{y}{\lambda}) \qquad (2\text{-}1)$$

where ω = radian frequency, k= 2π/λ, and λ is wavelength.

Per RHS of (1), (2-1) must be integrated over loop area in order to get flux. In Figure 3, infinitesimal area (da) equals (h dy), because h << λ (transmission line); i.e., $\underline{B}$ is constant over wire separation.

$$\phi = \int_{area} \underline{B} \bullet d\underline{a} = \int [B_O \sin(\omega t - ky)\, \underline{i} \bullet da\, \underline{i}]$$

$$= B_O \int [\sin(\omega t - ky) * h\, dy] \qquad (2\text{-}2)$$

where limits of integration for last integral expression of (2-2) are y running from 0 to l.

Evaluation yields

$$\phi = B_O \frac{h}{k} \quad [\cos(\omega t - kl) - \cos \omega t]. \qquad (2\text{-}3)$$

Time derivative of magnetic flux yields induced loop voltage.

$$V_i = \frac{d}{dt} [\oint \underline{B} \bullet d\underline{a}\,] = B_O \frac{h}{k} \frac{d}{dt} \quad [\cos(\omega t - kl) - \cos \omega t]$$

$$= B_O \frac{h}{k} \quad [-\omega \sin(\omega t - kl) + \omega \sin \omega t]. \qquad (2\text{-}4)$$

Common term may be factored out, and resultant coefficient term ω/k

= c, the speed of light. From B = μH, and traveling plane wave relation H = E/120π, (2-4) may be expressed as

$$V_i = \frac{c\,\mu}{120\pi}\ \ h\,E_o\,[-\sin(\omega t - kl) + \sin \omega t]. \qquad (2\text{-}5)$$

Simplification of leading constant terms in (2-5) yields

$$V_i = h\,E_o\,[-\sin(\omega t - kl) + \sin \omega t]. \qquad (2\text{-}6)$$

(2-6) is more appealing if we make a trigonometric substitution [$\sin\alpha - \sin\beta = 2\cos\frac{1}{2}(\alpha+\beta)\ \ \sin\frac{1}{2}(\alpha-\beta)$ ]. (2-6) becomes

$$V_i = 2h\,E_o[\cos\tfrac{1}{2}(2\omega t - kl)\ \ \sin\tfrac{1}{2}\ \ kl]. \qquad (2\text{-}7)$$

Time dependence is not important. At some time, induced voltage will be at a maximum, which occurs when cos (2ωt - kl)/2 = 1. Maximum induced voltage is (with k = 2π/λ):

$$V_i = 2h\,E_o \sin kl/2 \ = \ 2h\,E_o \sin \pi l/\lambda \qquad (2\text{-}8)$$

At low frequencies, where length is short relative to wavelength, small angle approximation holds (sin x = x for small x), and (2-8) reduces to

$$V_i = \ 2\pi l h\,E_o/\lambda \qquad (2\text{-}9)$$

At frequency where loop length is one-half wavelength, (2-9) reduces further to (substitute l = λ/2)

$$V_i = \pi h\,E_o \qquad (2\text{-}10)$$

This is a high frequency asymptote bounding induced potential at all frequencies above corner frequency defined by l = λ/2.

Now we have all information necessary. (2-8) is the accurate model, while (2-9) and (2-10) give a Bode plot approximation. Figure 4 plots all three equations.

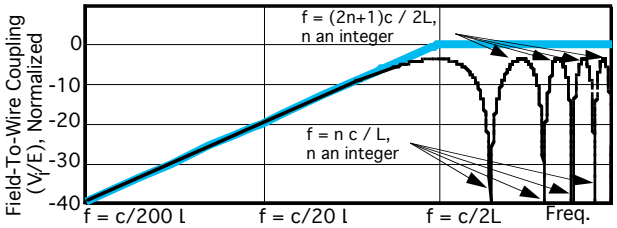


**Figure 4:** *Electromagnetic field-to-wire coupling vs. frequency*

Electric field coupling is discussed in a more intuitive fashion. Two electric field orientations are shown in Figure 5. Loop induced voltage ($V_i$) is given by integral around loop of dot product of electric field and loop perimeter:

$$V_i = \oint \underline{E} \bullet d\underline{l} \qquad (3\text{-}1)$$

When electric field is vertically polarized (Fig. 5a), Poynting vector, S, is directed along line length; wave travels down long dimension of transmission line. Line integral is evaluated around closed loop. Integral is broken up into four ordinary integrals (four sides of loop).

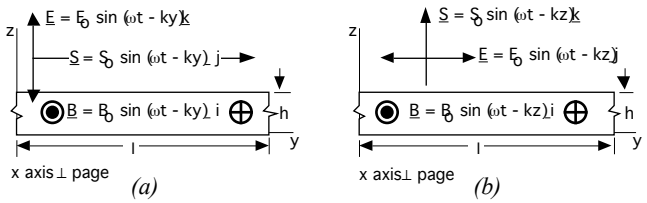


**Figure 5:** *Vert. (a) & horz. (b) polarized field-to-wire coupling*

First integral is evaluated from (0,0) to (0, h), where E-field is parallel to loop perimeter. Next integral is evaluated from (0,h) to (l,h), where E-field is perpendicular to loop perimeter with zero contribution. Third integral is evaluated from (l,h) to (l, 0), where E-field is parallel to loop height, but in opposite sense from first integral. Last integral, evaluated from (l,0) to origin is again zero.

$$V_i = \oint \underline{E} \bullet d\underline{l} = \int_0^h E_o \sin(\omega t - ky)\,\underline{k} \bullet \underline{k}\,dz + 0 + \int_h^0 E_o \sin(\omega t - ky)\,\underline{k} \bullet \underline{k}\,dz + 0. \qquad (3\text{-}2)$$

In both non-zero integrands, trigonometric expression is independent of variable of integration. Result of each integration process is integrand multiplied by loop height. (In non-zero integrands, equal coupling occurs, except for a phase factor due to time interval required to traverse line length. This is why a dc field cannot couple to a loop, and why coupling increases with increasing frequency.)

$$\int_0^h E_o \sin(\omega t)\,\underline{k} \bullet \underline{k}\,dz = h\,E_o \sin(\omega t) \qquad (3\text{-}4)$$

$$\int_h^0 E_o \sin(\omega t - kl)\,\underline{k} \bullet \underline{k}\,dz = -h\,E_o \sin(\omega t - kl) \qquad (3\text{-}5)$$

Then,

$$V_i = \oint \underline{E} \bullet d\underline{l} = h\,E_o \sin(\omega t) - h\,E_o \sin(\omega t - kl)$$
$$= h\,E_o\,[\sin(\omega t) - \sin(\omega t - kl)]. \qquad (3\text{-}6)$$

(3-6) is equivalent to (2-6), and same conclusion follows.

Direct analysis of horizontal electric FTW coupling follows form of vertically polarized case, with one exception. Figure 5b shows field orientation relative to transmission line when electric field is parallel to transmission line long dimension (horizontal pol-arization) *and* magnetic field penetrates plane of loop. In vertical case, coupling occurs along height of transmission line, which is electrically short by definition. Therefore, limit of integration is line height. As discussed above, phase difference accounts for coupling efficiency. In the case of horizontal polarization, Poyn-ting vector is parallel to line height and phase factor is always small. Coupling is to (arbitrarily long) line length. While line length, l, is limit of integration, it only yields maximum coupling when l< λ/2. When length exceeds λ/2, λ/2 or odd multiples thereof provide maximum coupling. This is somewhat intuitive, since once the first half wavelength has coupled, contribution from next half is in opposite polarity and decreases coupled potential, as illustrated in Figure 6. (Integrating areas under Fig. 6 loops yields Fig. 4 graph.) Smith also shows that results (2-8) - (2-10) and Figure 4 apply equally when electric field is polarized along transmission line length, as long as magnetic field penetrates plane of loop. Note that in this case, evaluation of (3-1) along a resonant line length can result in a large end-to-end potential; hence, large currents flow along conductors, i.e., large *antenna* currents may therefore be induced on transmission line conductors. However, except for a small phase factor, such currents induce equal potentials in each side of line, hence same small *loop* current as couples under vertical polarization.

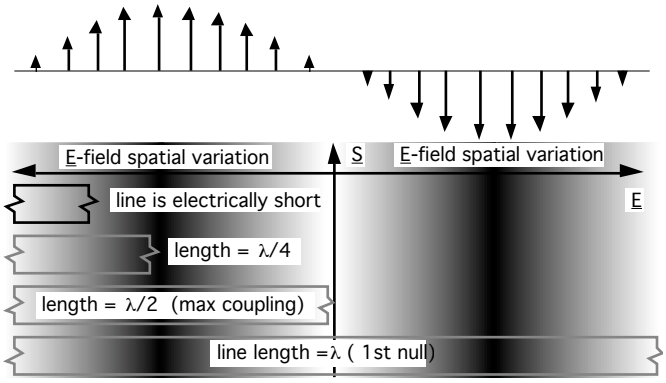


**Figure 6:** *Horizontally polarized E- field intensity along loop*

If magnetic field does *not* penetrate plane of loop, then (1) says no net loop potential is coupled. If in Fig. 5b assignment of S and B vectors is interchanged, with S penetrating plane of loop, then identical electric field coupling occurs to both transmission line conductors. Potential induced across either end, regardless of

magnitude of coupling to line length, is zero. This means that there is no relationship between line-coupled antenna currents and transmission line-connected victim potentials. This is important when assessing RI/CI correspondence.

Figure 7 shows theoretical and measured em FTW coupling. Field illumination is vertical. Field source is a 15 cm high parallel plate of 90 Ω characteristic impedance. It is plate described by Trout (1996), but matching networks are redesigned, and although plate is designed for use up to 200 MHz, correcting for plate and matching network losses allows good correlation of field intensity and coupling to 700 MHz.

Illuminated transmission line consisted of 16" long AWG 10 wire mounted 1.7" above ground. Material supporting wire had a relative permittivity of 5, which increased electrical length to 36". Characteristic resistance was 180 Ω. Figure 7 data is attenuated by resistive matching losses to a 50 Ω spectrum analyzer.

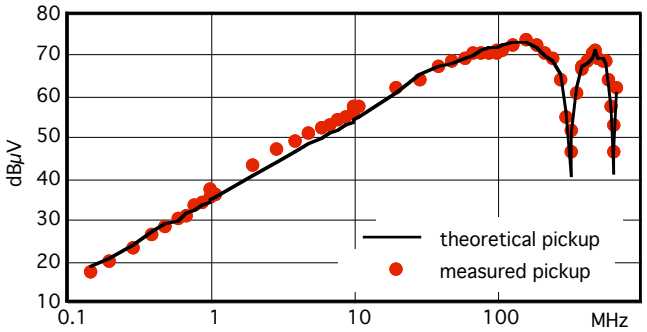


**Figure 7:** *Theoretical and experimental field-to-wire coupling*

***Modeling Field-To-Wire Coupled Potentials***

An important subject not addressed in foregoing analyses is line-coupled potential modeling. Electric field coupled potential is in shunt, that is, in parallel with transmission line source and load impedance, whereas magnetic coupled potentials inject in series between loads. Figure 8 shows a lumped-element model of these sources in a transmission line. The distinction is immaterial in a matched transmission line, or even an unmatched line, with fairly symmetrical loads. But if termination impedances differ significantly, or if illuminating field is strongly electric or magnetic, shunt/series nature is apparent. Figure 9 shows a test set up used to measure the effect on FTW coupled potentials of different field and swag termination impedances. Wire is 30" long, 1" above a ground plane, and exposed to a vertically polarized field under a parallel plate. Wire is terminated in spectrum analyzer (50 Ω) at one end and sc, oc, or 50 Ω impedance at far end. Data taken at 1 MHz unless otherwise noted, -10 dBm driving plate except as noted. Plate load varied to give different em field impedances. (In both open and short circuit loading of plate, drive was reduced 6 dB to -16 dBm, in order to maintain respectively plate potential and plate current at identical levels to plane wave exposure. In so doing, plate current drops with an open circuit, and plate potential drops with a short circuit.)

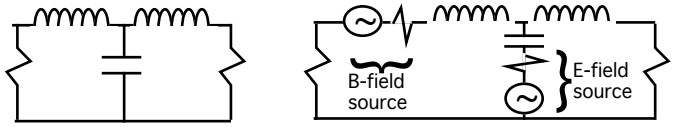


**Figure 8:** *Lumped-element model of lossless transmission line with and without coupled potentials*

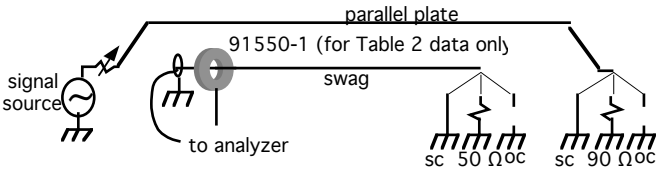


**Figure 9:** *FTW coupling as a function of field & wire impedance*

Table 1 presents FTW coupling versus line load impedance. There is almost no difference in coupled potential when a plane wave illuminates either symmetrically loaded line, or line with far end shorted. While shorted end loads electric coupling mechanism, magnetically induced potential drops more potential across remaining impedance. When a plane wave illuminates a 50 Ω/oc line, electric coupling can supply a higher potential, but series magnetic source is all dropped across open circuit.

**Table 1: Field -To-Wire Coupling As A Function Of Wire Loads And Field Impedance**

| Plate Load/ | Pick-up (dBμV) vs. loading | | |
|---|---|---|---|
| field impedance | 50 Ω/ sc | 50Ω / 50Ω | 50 Ω / oc |
| matched/377 Ω plane | 43 | 42 | 35 |
| shorted (sc)/magnetic | 49 | 42 | 5 |
| open circuit (oc)/electric 2 MHz | 33 | 36 | 40 |
| open circuit (oc)/electric 1 MHz | 23 | 29 | 33 |
| oc /electric 0.5 MHz | 10 | 22 | 26 |

With highly magnetic illumination, series coupled potential dominates. Therefore, potential at 50 Ω load doubles when other end is short-circuited, and almost disappears when opposite end is open-circuited. Inspection of behavior of coupled potentials under a high impedance electric field is clearest at low frequen-cies. At 500 kHz a short circuited line drops coupled potential at 50 Ω end 12 dB, while an open circuited end causes a 4 dB increase (all relative to a 50 Ω/50 Ω condition). At higher frequencies (1 and 2 MHz), same effect is noted but less extreme (more displacement current flows in plate at these frequencies), field is not as strongly electric.

Having determined, analytically, maximum coupling to a transmission line, the following section proceeds to inject calculated values by conducted means.

## CONDUCTED INJECTION TECHNIQUES

Treatment here is not introductory. It assumes reader is familiar with current clamp injectors, used for bulk current injection (BCI), coupler/decoupler networks, described in IEC 1000-4-6, and the electromagnetic clamp also described in that standard. These devices are discussed in terms of their ability to inject signals into a CUT, and the degree of correspondence of injected and radiated coupling.

Both current clamp and electromagnetic clamp are non-intrusive methods of injecting signals into bundles. A CDN is inserted into bundle. Either clamp method injects in series with CUT, CDN injects in shunt, between ground and CUT. Models are shown in Figure 10.

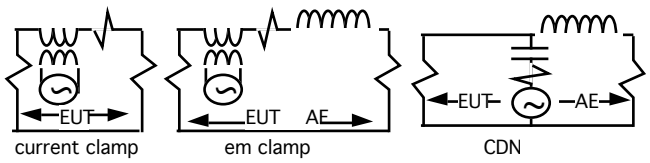


**Figure 10:** *Modeling conducted injection*

Comparison of Figures 8 and 10 shows that clamp injection models magnetic, while CDN injection models electric field coupling. Note, however, that em clamp and CDN add an extra feature unavailable with current clamp injection: directionality/ isolation. With latter two techniques, tester can choose which circuit is under test (EUT versus

auxiliary equipment - AE). With em clamp, above ≈25 MHz, signal injected into EUT is independent of AE impedance. This is true of entire frequency range for CDN (150 kHz - up).

Isolation provided in latter two techniques assures that desired signal can be driven into CUT, regardless of AE impedance. What is effect of AE impedance when using a current clamp? Table 2 lists BCI clamp power input required to drive same currents and couple same potentials induced on a swag per Figure 9 but with Figure 11 set up. Plate was matched with 90 Ω and driven at 10 dBm at low frequencies, and at 0 dBm above 1 MHz. Swag voltage and current were measured from 150 kHz to 100 MHz as a function of opposite end impedance. As shown in Figure 11, wire was then driven with a current clamp, such that same current flowed on wire as during radiated illumination. Wire potential was measured when current clamp induced current was same as radiated induced. Current probe was never moved from a position adjacent to spectrum analyzer end of wire during these tests and current clamp was in a fixed position adjacent to current probe. Because normal BCI test technique has power precalibrated in a 50 Ω/50 Ω circuit, deviation of power noted below from that shown for 50 Ω/ 50 Ω situation is a measure of non-ideality of current clamp injection technique. (Table 2 data normalized to a constant 0 dBm plate drive.) Table 2 data entries make clear that pre-calibration of current clamp power into 50 Ω/50 Ω circuit suffices reasonably for 50 Ω/sc case, but provides poor correlation when AE load is oc. Correlation improves with increasing frequency, since, electrically speaking, oc is further away.

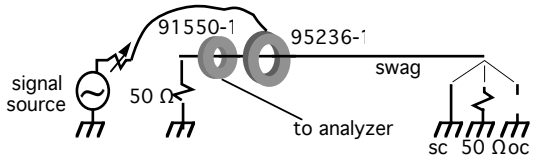


**Figure 11:** *Using clamp to inject currents measured in figure 9*

**Table 2: BCI Clamp Input Power Vs. CUT Load Impedance (With FTW Coupling As A Baseline)**

| Freq. (MHz) | 50Ω/50Ω dBm | 50Ω/oc dBm | 50Ω/sc dBm |
|---|---|---|---|
| 0.3 | -63 | -28 | –64 |
| 1 | -53 | -24 | -54.5 |
| 3 | -41 | -22 | -42.5 |
| 10 | -30.4 | -20 | -31 |
| 30 | -20 | -19 | -22 |
| 100 | -4 | -13 | 2.5 |

With this background in FTW coupling physics and techniques available for CI, objections raised against CI techniques may now be evaluated.

## CI TECHNIQUES: CRITICISM AND REBUTTAL

Objection 1. FTW coupling is a distributed phenomenon which is not accurately modeled by a lumped-element method. Adams (experimental) and Perini (method of moments) demonstrated large (40+ dB) differences between RI and CI techniques.

Reply. CI techniques *are* lumped-element models of a distributed FTW coupling phenomenon. As such, one would expect best correlation at low frequencies, with degraded fidelity as CUT length approaches λ/2. In this context, it is interesting to compare the work of Adams, Perini, and Trout. Adams tested from 20 - 150 MHz, on wires at least 3 meters long routed inside a helicopter frame, while Perini (1995A,B) predicted current flow on a 0.6 m long transmission line at 10, 100, and 300 MHz. Adams' procedure was to measure illumination-induced bulk cable cur-rent on an entire bundle, as a function of frequency, as well as currents flowing on individual wires making up the bundle. Then previously measured bulk cable current was *injected* into cable, and individual wire pair currents were compared to that measured during illumination. Adams showed 40 dB disparities. Given Adams' setup, this is expected.[2] Trout's technique followed Adams', but strove for even illumination and low frequency. Trout, using parallel plate described herein, illuminated 1 m long wires and found ±2 dB correlation from 100 kHz to 80 MHz. Perini showed large disparities analytically at 100 and 300 MHz, but 4 dB correlation at 10 MHz where wire was electrically short.

It has never been argued that CI techniques are accurate at high frequencies. Using high frequency test results to condemn the technique ignores its utility, which is to adequately stress a CUT at low frequencies, when this is impossible to do with a radiated field. Further, per test philosophy introduced at beginning, it is unimportant to precisely reproduce RI effects with a CI technique, it is sufficient merely to produce a worst case stress. This is exactly why CI limits have curves such as Bode plot asymptotes of Figure 4, rather than node/anti-node exact response.

Objection 2. Parallel plate type illumination of transmission line (vertically polarized) is not worst case: horizontal polarization yields more efficient coupling. (Trout's work was criticized for using vertical polarization.)

Reply. FTW coupling physics discussion explains this is not so when victim CUT can be modeled as a swag, i.e., when EUT is slated for platform installation. Maximum coupling to trans-mission line loads occurs with magnetic field perpendicular to plane of loop, regardless of electric field polarization (subject to $\underline{S} = \underline{E} \times \underline{H}$). Objection statement may be true sometimes for Figure 1a condition, but rarely, if ever, for platform installations (Figure 1b). It is true that horizontal $\underline{E}$-field polarization with $\underline{S}$ pene-trating loop plane (Figure 5b with $\underline{S}$ and $\underline{B}$ interchanged) can yield tuned-dipole like current distributions along transmission line length. These *antenna currents*, however, do not contribute to load-coupled potential; antenna currents vanish at ends of transmission line. Smith (1977) sections 1.3 & 1.4 provide ana-lytical treatment with same conclusion. When measuring CUT-coupled currents under low-level illumination, probe is always placed within a fraction of a wavelength of victim load of interest. Current at other places along line is not important. It is an error to use antenna currents as a fundamental indicator of FTW coup-ling; it is transmission line load coupling that is of interest.[3]

Objection 3. Use of equation (1) and various subsets to compute FTW coupling does not account for effect of currents flowing on transmission line. (This is closely related to items 1 & 2 above.) Perini cites Weeks (1968) and uses

$$V_{oc} = \frac{1}{I_o} \int \underline{I}_T \bullet \underline{E}^I \, dl \qquad (4)$$

where $V_{oc}$ = open circuit potential available at antenna port,

$I_T$ = antenna current developed when port is fed $I_o$, and

$E^I$ = incident field intensity in absence of antenna

Reply. Objection is valid for test set up of Figure 1a when CUT is electrically long, invalid for Figure 1b set up. Following discussion is confined to showing that (3-1) is an acceptable substitute for (4) under Figure 1b conditions. Any antenna which efficiently transduces Poynting vector power density into power flowing in a guided wave (transmission line) must be described per (4). A passive antenna with a non-vanishing effective aperture operates in a resonance mode, where antenna currents differ greatly along antenna physical aperture, and from output current. In a transmission line, however, at low frequencies, currents are everywhere nearly identical. Under low frequency conditions, then, (4) clearly reduces to (3-1). Condition defining low frequency operation is (5), relating transmission line input to load impedance. As long as these are close, i.e., kl is small, (3-1) is a reasonable approximation of (4).

$$\frac{Z_{input}}{R_c} = \frac{Z_{load} + j\, R_c \tan kl}{R_c + j\, Z_{load} \tan kl} \quad , (R_c = \text{characteristic resistance}) \quad (5)$$

These issues aside, equal length tuned dipoles and transmission lines have a definite effective height ($h_e$) relationship. $h_e$ is defined as the ratio of antenna port voltage to electric field intensity. For a tuned dipole driving a matched load, $h_e$ is $\lambda/2\pi$. From (2-10) maximum transmission line (loop) $h_e$ is $\pi$•wire separation. Wire separation in a transmission line is, by defini-tion, small relative to wavelength.[4] Therefore, ratio of dipole and transmission line $h_e$ is a large number, meaning that a dipole draws much more power from a field than an equal length transmission line. These mathematical arguments are bolstered by the intuitive approach developed in the FTW physics section. Consider transmission line conductors as two dipoles in close proximity. Given an incident field parallel to these conductors (Figure 5b), at resonance a large potential difference can build up from end-to-end, driving large resonant currents. But very nearly the same potential difference is developed across both dipoles making up the transmission line. Only phase difference due to time lag traversing distance between wires accounts for a net potential difference across transmission line loads. Therefore, loop to antenna current ratio is small. *While (4) is necessary to describe antenna currents, (1) is sufficient to describe loop current flow; hence, victim coupling.* Loop currents are equal and opposite, and are in close proximity, so field disturbance due to loop currents is minimal relative to a single dipole alone, or to transmission line antenna currents. An experiment was designed to demonstrate these facts. A transmission line and dipole of same physical length (~15") were constructed. Both were exposed to plane wave illumination in EMC Integrity's IEC 1000-4-3 ferrite tile-lined anechoic chamber, where field uniformity over 15" was typically 0.2 dB, but no greater than 0.6 dB. Electrically short field strength sensors of type required for 1000-4-3 quiet zone calibration were placed in immediate vicinity of dipole and transmission line, as shown in Figure 12a (dipole not shown). Field sensor readings were taken at positions shown. Readings were compared to those for empty quiet zone. Horizontal dipole and transmission line were found (at resonance) to load horizontally polarized field at their centers by as much as 6 dB. At ends, field intensity was boosted by 2 dB. This is intuitively appealing: resonant current flows in middle of dipole so as to oppose field which induced it; high potentials developed at dipole ends boost field intensity in immediate vicinity.

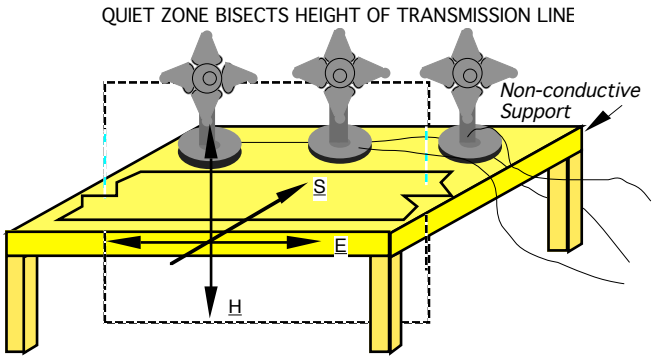


**Figure 12a:** *Horizontal E-field disturbance measurement*

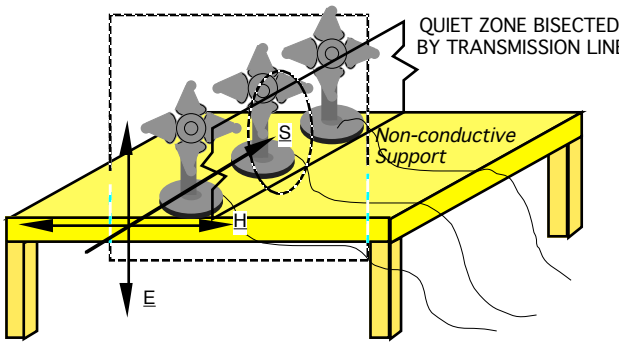


**Figure 12b:** *Vertical E-field disturbance measurement*

In contrast, when same transmission line was exposed to vertical polarization and oriented for maximum pick-up per Figure 12b, field disturbance was less than 1.7 dB. *Transmission line load-coupled potentials do not disturb incident field and (3-1) is a suitable replacement for (4).*

Another test performed in an outdoor open area demonstrated how vertical and horizontal polarization and transmission line orien-tation effect antenna/loop current distribution on transmission lines. Table 3 summarizes results.[5] A 30 - 1000 MHz modified bowtie antenna (6 m distant) illuminated an 18" transmission line at its tuned frequency of 328 MHz per Figures 13a & 13b. Induced currents were measured at transmission line midpoint and loads. With E-field vertically polarized per Figure 13a, current at midpoint and loads was within 5 dB. Placement of current probe around both transmission line conductors showed that current flowed around loop (measured net current in both conductors was 12 dB below that in a single conductor).

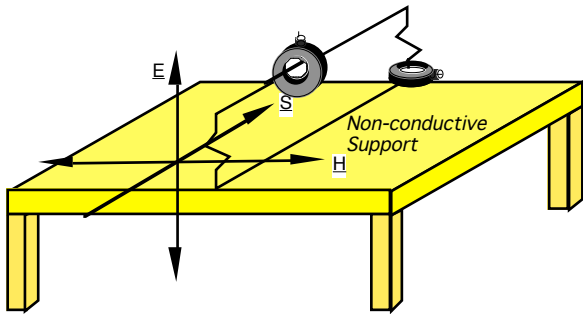


**Figure 13a:** *Measurement of transmission line induced current due to vertically polarized E-field*

With horizontal polarization per Figure 13b, midpoint current was 22 dB above load currents. Placement of current probe around both transmission line conductors confirmed that mid-point current was antenna in nature; net current in both conductors was 5 dB above that in an individual conductor. In Figure 13b set up, load current was within 2 dB of that measured in loads of Figure 13a set up; that is, near equal *loop* coupling was measured for both orientations and polarizations.

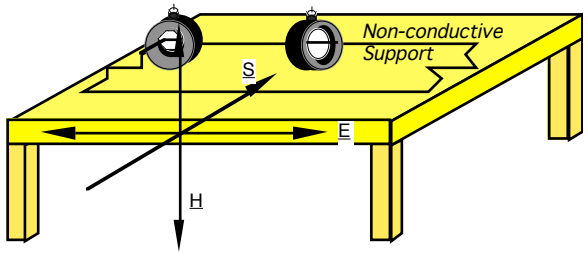


**Figure 13b:** *Measurement of transmission line induced current due to horizontally polarized E-field*

**Table 3: Current Coupling To Transmission Line As A Function Of Polarization**

| E-field polarization | 94106-1 dBμV from below positions | | |
|---|---|---|---|
| | center | both center conductors (antenna current) | load |
| Horizontal | 60 | 65 | 38 |
| Vertical | 45 | 33 | 40 |

Objection 4. Use of BCI techniques for low-level illumination and scaling up to higher threat levels is only valid for linear and reciprocal circuits. If a circuit characteristic is non-linear with respect to applied stress level, then low-level stress application and linear scaling is inaccurate.

Reply. Low-level illumination of aircraft, measurement of accompanying induced cable loop current; scaling for illumination field intensity relative to full threat, and injecting or comparing scaled cable loop current to specified levels has become an accepted practice for certifying aircraft avionics suites to both lightning and high intensity radiated field (HIRF) environments (Carter, 1990). Concern that a circuit might demonstrate non-linear behavior over a dynamic range that may include a 1 V/m low-level illumination and a 200 V/m threat is warranted if cable induced differential mode (dm) current is monitored on a single circuit. But this is never the case. It is loop or bulk current (hence acronym - BCI) in entire bundle, inherently cm in nature, that is monitored. Bulk current coupled to a CUT depends not on individual circuit dm impedance, but on shield terminations and parasitic capacities from each wire to structure. This is illustrated by a simple test. 30" long RG-58 coax, shield grounded at each end, is parallel plate illuminated. A current probe measures loop current flowing as a result. Load at each end of coax is either sc or oc. Inspection of Figure 14 reveals identical currents regardless of termination impedance.

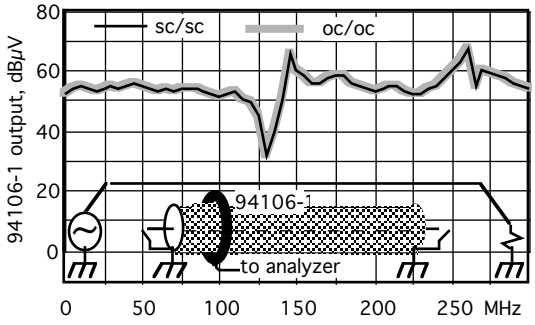


**Figure 14:** *Induced current as a function of load impedance*

Objection 5. On a multi-conductor bundle, a CI technique will not yield good fidelity relative to radiated illumination.

Reply. Given an unshielded multiconductor cable, with well defined inner and outer wire paths, one would expect that, above and beyond current splitting among various conductors, outer wires shield inner wires by virtue of a skin depth-like phenomena where induced currents tend to ride on outer edge of bundle. Certainly a CDN injection approach will not simulate this effect; the whole purpose of a CDN being to inject equal potentials on all cable conductors. However, BCI approach is quite satisfactory in simulating the illuminated response. A test analogous to Adams and Trout was designed. A 3' unshielded cable had 34 individual conductors (17 twisted pairs) each wire terminated to connector shell through 50 Ω. Figure 15 shows cross-sectional geometry of cable, as well as cable termination using 50 pin D-style connectors. Two wires, one each at periphery and center, were terminated at one end in a bnc connector, for connection to a spectrum analyzer. Connectors at either end were connected to ground plane, and illuminated under a parallel plate. A current probe measured cable loop current. Both loop current and voltage pick-up were measured. Next, a BCI clamp was driven to induce previously measured loop current and voltage pick-up was monitored and compared to that measured under parallel plate. Figure 16 shows test results from 150 kHz to 110 MHz. Close agreement is attained to 60 MHz (above 60 MHz plane wave coupling is also poorly behaved). CUT is λ/5 at 60 MHz. In this case BCI is clearly superior to CDN injection technique.

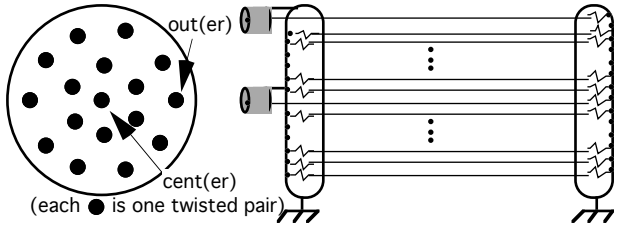


**Figure 15:** *Cross-section of multiconductor cable, and termination/instrumentation of individual conductors*

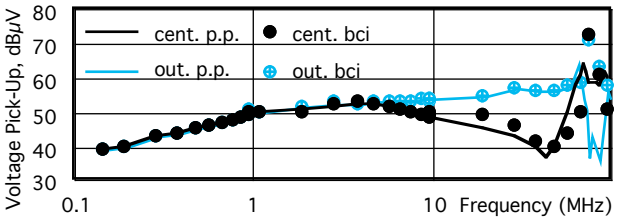


**Figure 16:** *Coupling to multiconductor cable*

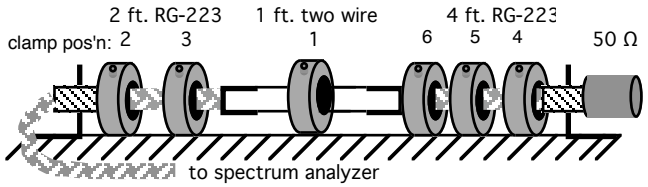


**Figure 17a:** *Test set up to measure pick-up as a function of clamp vs. shield break position*

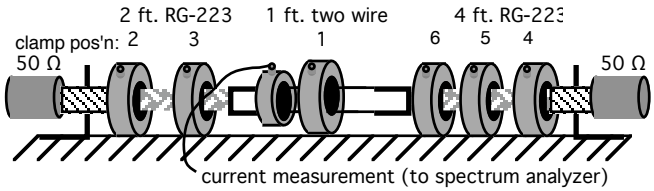


**Figure 17b:** *Measuring current as a function of clamp position*

Objection 6. When CI testing a shielded bundle, coupling will depend strongly on whether coupling device is placed at a weak point of the shield. This is not the case for the distributed phenomenon of radiated illumination.

Reply. Voltage pick-up dependence on distance of lumped-element injector from a shield discontinuity is not as pronounced as on position of current maximum relative to shield discontinu-ity. Figure 17a shows a 7' transmission line made of two pieces of RG-223 coax, 2' and 4' long, and a 1' section of two-wire line. Large break was used so that effects would be obvious at low frequency. Two-wire break was placed in two different positions: at one end and in between two coax sections. Figure 17b shows a current probe placed at two-wire section center. A current clamp was placed in numerous positions along length of 7' cable and pick-up at one end of wire was measured with a spectrum analyzer (other end terminated in 50 Ω dummy load). Figures 17a&b show shield break at center set up.

Figure 18a shows clamp placement at break is no guarantee of maximum coupling; Figure 18b shows stronger correlation between maximum pick-up and current maxima at shield break. In a similar test, a more realistic two-wire shield break 2" long was made between two pieces of RG-223 coax. End-to-end assembly was 30" long, 1" above ground. Figures 19a&b show test set up. Technique again compares parallel plate induced to BCI coupling. Voltage pick-up and loop current were measured under parallel plate. Recorded currents were then induced via BCI. Voltage pick-up was compared to that previously recorded. Current was measured both at cable end, per normal technique, and at shield break. Injection was at cable end, per normal technique, and at shield break. Figure 20 demon-strates that standard practices for current probe/clamp placement yield acceptable results to 125 MHz, which was λ/3 in this test.

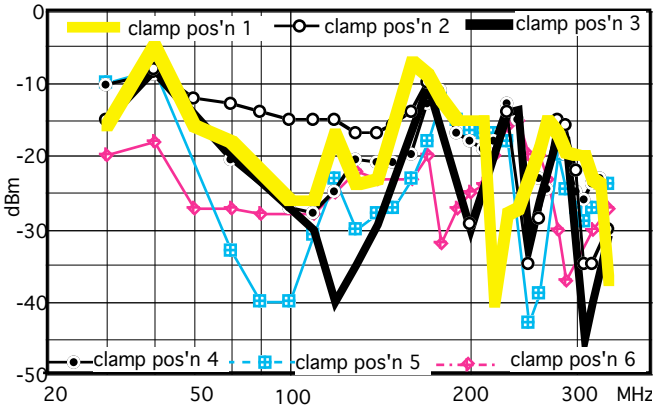


**Figure 18a:** *Pick-up as a function of clamp vs. shield break pos'n*

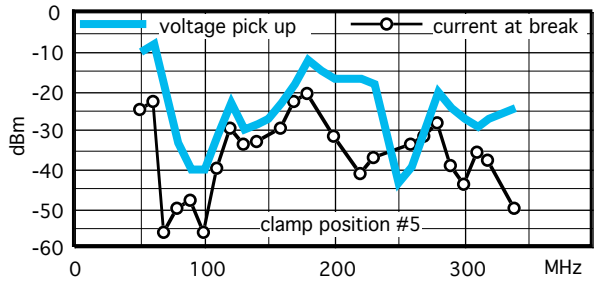


**Figure 18b:** *Pick-up vs. current at shield break (typical)*

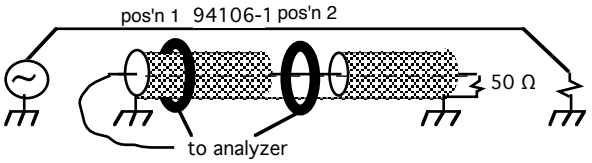


*a) FTW test set up*

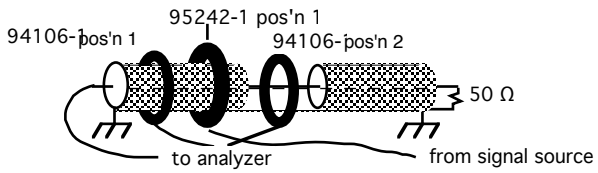


*b) BCI test set up*

**Figure 19:** *Measurement of FTW vs. BCI coupling to shield break*

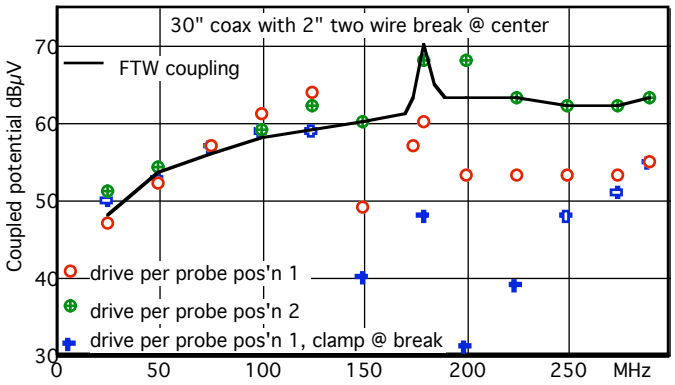


**Figure 20:** *FTW vs. BCI coupling to coax with shield break*

Related experiments illustrate another link between CI and RI testing. Set up of Figure 17a was used, except no shield break was present. Four clamp positions were used: one at each end and two evenly spaced between. Figure 21 graphs pick-up as a function of clamp position. *It is clear that sliding a BCI clamp up and down the CUT is tantamount to mode-stirring a reverberant chamber.*

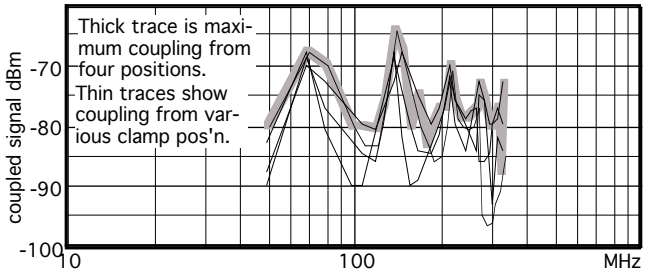


**Figure 21:** *Effect of moving clamp along line (mode-stirring)*

In Figure 21, few "paddle positions" are charted. Finer clamp spacing steps (degrees per step of paddle rotation) will yield maximum stress of CUT loads. This is shown in Figure 22, where test set up was that of Figure 19, but without shield break.

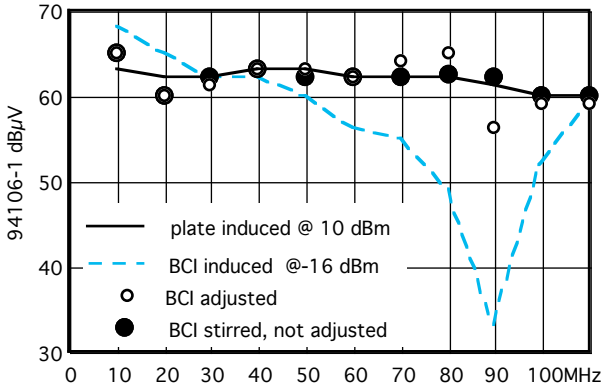


**Figure 22:** *Smoothing effect of BCI "mode-stirring"*

FTW coupling provides smooth response, but BCI clamp, driven at a near constant level (based on relatively smooth insertion loss as calibrated in 50 Ω system) shows a large null at 90 MHz. This can be overcome by driving clamp harder (BCI adjusted), but in general this is not done. Placing clamp at three positions spaced 12" apart along coax CUT results in BCI stirred mode data points, using near constant input to clamp. Such a mode-stirred result is exactly what is desired per the test philosophy section: maximum or worst case stress, not direct replication of nodes and anti-nodes.[6] But, as seen in Figure 22, sliding a BCI clamp has one tremendous advantage over mode-stirring; it does not create the large number of modes and

hence the multiplied stress level of a mode-stirred chamber. No adjustment need be made to induced stress levels while sliding the clamp. The only disadvantage is that shared with mode-stirring: increased test time. However, schedule impact is not as severe at lower frequencies associated with CI testing. Only two extra positions were required to get smooth response of Figure 22. Consider IEC 1000-4-6 0.15 - 80 MHz, 9 octave frequency range. Lumped-element modeling is adequate when circuit length is λ/7.5 or less. For IEC-1000-4-3, CUTs appear to be (generally) limited in length to 1 m. See Figure 23 in reference to following discussion. 1 m is λ/7.5 at 40 MHz. So from 0.15 - 40 MHz, a single injection point (A) is required. From 40 -80 MHz, extra injection points (multiples of λ/7.5 away at 80 MHz, or 0.5 m (B) and 1 m (C)) are required. Assuming, per IEC 1000-4-6, equal dwell time per octave, extra required testing to assure maximum coupling requires 22% of original test time. (λ/7.5 and multiples thereof chosen for convenience, working with 1 m CUT and 80 MHz frequency range. λ/10 is more common low frequency boundary, but results in more complex procedure.)

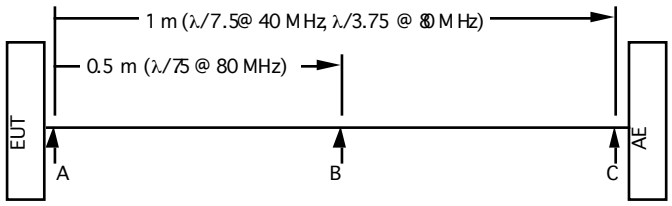


**Figure 23:** *Multiple clamp positions*

Objection 7. A non-reciprocal circuit element (e.g., an amplifier) will yield different results with stresses applied to input versus output. CI techniques check only one bundle at a time, whereas radiated illumination provides simultaneous stimulation.

Reply. In vast majority of cases, it is sufficient to test one CUT at a time. In rare cases, such as redundant circuits that feed redun-dant flight computers which "vote" based on respective data in-puts, it may be necessary to simultaneously excite all CUTs. This is because despite redundancy, it might be expected that entire aircraft is illuminated and all cables excited. Clearly, injecting simultaneously on several CUTs is complex and a radiated test provides effortless simultaneous illumination. But in frequency bands where it is impossible to adequately stress CUTs via illumination, there is no choice except simultaneous injection.

## CONCLUSION

Conducted immunity techniques were developed to overcome illumination spot size, field uniformity, antenna efficiency, and rf power limitations inherent in radiated immunity testing at low frequencies. Since CI methods were introduced, criticism has been levied as to the fidelity with which these techniques repro-duce electromagnetic field-to-wire coupling. This paper showed on practical, as well as philosophical and theoretical grounds, that CI testing is a valid tool for modeling field-to-wire coupling at frequencies where transmission line or antenna effects are mini-mal. In developing the physics of field-to-wire coupling, several important concepts were introduced. Among these are the neces-sity of differentiating between antenna and loop current, and the differing nature of electric and magnetic field-to-wire coupling. With this background, seven criticisms, or objections to conduc-ted injection techniques, were examined and explained to be examples of limited applicability, in no way condemning the overall validity and utility of the conducted immunity concept. In addressing these seven objections, this paper presented and integrated into an overall picture the separate efforts of Adams, Perini and Trout, each of whom have previously produced valuable critiques and commentaries on the subject of this paper.

## ACKNOWLEDGMENTS

The author wishes to thank the following colleagues and companies for their invaluable assistance. Many theoretical and test-related discussions with Mark Nave of EMC Services were instru-mental in successfully completing this effort. Vincent Greb of EMC Integrity in Longmont, Colorado measured field disturbance due to transmission line and antenna currents in an EMCI anechoic chamber. The chamber's quiet zone provides exceptionally even illumination, not only in the quiet zone plane, but perpendicular to it. EMCI measurements were crucial in showing that a transmission line oriented for maximum coupling from a vertically polarized field did not disturb the field, but when oriented for maximum coupling from a horizontally polarized field, loaded the field significantly. This experiment provided the basis for differentiating between antenna and loop currents. Long term loan of Farnell and Tegam rf test equipment made this work possible. Errors are solely the author's responsibility.

## REFERENCES

Szentkuti, B., Give Up Radiation Testing In Favour Of Conduction Testing, *Proceedings, EMC* Zurich 1989.

Adams, J. and Melquist, D., "Comparison Measurements of Currents Induced by Radiation and Injection," *IEEE Transactions on Electromagnetic Compatibility*, vol. EMC-34, no.3, p. 360-362, August 1992.

Trout, D., "Investigation of the Bulk Current Injection Technique by Comparison to Induced Currents from Radiated Electromagnetic Fields," *1996 IEEE EMC Symposium*, Santa Clara, p. 412-417.

Perini, J., "Radiated Versus Injected measurements: When Are They Equivalent?", *Proceedings 10th International Symposium on EMC,* March 9 - 11, 1993, Zurich, Switzerland, p. 343-348.

Perini, J., Cohen, L. S., "Radiated Versus Injected measurements: When Are They Equivalent? - Part 2", *Proceedings 11th International Symposium on EMC*, March 6 - 8, 1995, Zurich, Switzerland

Perini, J., Cohen, L. S., "On The Equivalence Of Radiated And Injected Tests", *1995 IEEE EMC Symposium,* 1995, Atlanta, p. 77-80.

Smith, A. A., "Coupling Of External Electromagnetic Fields To Transmission Lines," *Wiley-Interscience*, New York, 1977.

IEC 1000-4-6 1996-03 Immunity to conducted disturbances, induced by radio-frequency fields

Weeks, W.L., "Antenna Engineering," *McGraw-Hill*, NY, 1968, pp. 294-296.

Carter, N.J., "The Application of Low Level Swept RF Illumination as a Technique to Aid Aircraft EMC Clearance," *ITEM*, 1990.

## NOTES

[1] i, j, and k unit vectors represent, respectively, x, y, and z axes.

[2] If Adams' antenna or wiring were moved slightly, large disparities would again be expected. Given Adams' setup, Szentkuti may be paraphrased by saying that sometimes not even a radiated test equals a radiated test.

[3] If coupling is to a cable shield, then current is more important, through mechanism of shield transfer impedance. But it is not a fundamental issue. If CUT is resonant at VHF and above, an RI test will stress it, and if cable is long, only a CI test can begin to adequately stress it. It may be that such a cable should be driven a little harder than loop coupling calculations would indicate.

[4] It is this criterion that differentiates Figures 1a & b.

[5] Placement of current probe around transmission line disturbs currents, adding a cm factor, as evidenced by current flowing on coax between probe and spectrum analyzer. Table 3 results would be even better if a less disruptive measurement had been used.

[6] IEC 1000-4-6 attempts to control resonances by placing CDN within a confined region close to EUT. This is sufficient for an unshielded cable, but does not adequately stress a shielded bundle, since coupling through shield is related to shield leakage inductance, which varies directly with exposed cable length. Shielded cables should have entire length exposed to stress.